Phytochemistry 179 (2020) 112502

Contents lists available at ScienceDirect

Phytochemistry

journal homepage: www.elsevier.com/locate/phytochem

Glucosinolate catabolism during postharvest drying determines the ratio of bioactive macamides to deaminated benzenoids in *Lepidium meyenii* (maca) root flour

Eliana Esparza, Winnie Yi, Fabian Limonchi, Eric G. Cosio *

Chemistry Section and Institute for the Sciences of Nature, Earth and Energy (INTE-PUCP), Pontifical Catholic University of Peru, Av. Universitaria, 1801, Lima, 15088, Peru

ARTICLE INFO

Keywords:
Lepidium meyenii
Brassicaceae
Maca
Benzenoid metabolism
Glucosinolate hydrolysis
Postharvest processing
Benzyl alkamides
Aldehyde dehydrogenase
Amine oxidases

ABSTRACT

Postharvest processing of maca (*Lepidium meyenii* Walp., Brassicaceae), a traditional high-altitude Andean root crop, involves slow field drying prior to milling into flour. The progressive tissue dehydration and release of hydrolytic enzymes and substrates from cellular compartments results in the slow accumulation of free monosaccharides, fatty acids and amino acids. A more complex, and faster, kinetic profile is that of glucosinolate breakdown. A number of reactive transient and stable accumulation products are generated during drying, some of which have noteworthy bioactive properties. Among these are macamides, inhibitors of endocannabinoid neurotransmitter degradation in mammalian nervous systems. They result from the condensation of benzyl amine, a glucosinolate hydrolysis product, with free fatty acids released from lipid hydrolysis. Recent research has focused on developing drying processes under controlled conditions that can modulate the biochemistry of glucosinolate hydrolysis to optimize the content of bioactive compounds in the root flour. Low temperature (35 °C) oven-drying of shredded maca roots under controlled air flow generates benzyl amine as primary accumulation product, accounting for up to 94% of hydrolyzed glucosinolate in the flour. Kinetic evidence suggests that both deaminated benzenoids and macamides are allocated from the benzylamine pool through amine oxidase activity or condensation with free fatty acids, accounting for the remaining hydrolyzed glucosinolate (<5%). These activities determine the allocation to either one of these pathways. Later stages of dehydration result in shifts in the molar ratios of deaminated benzenoids, the accumulation of benzoic acid esters and benzyl alcohol. We propose that these are the result of changes in the rates of the reductive and oxidative half-reactions of endogenous aldehyde dehydrogenases. It is the ratio of benzylamine deamination to amide formation that determines the eventual yields of macamides in relation to benzenoids and their esters in maca flour.

1. Introduction

Postharvest processing of many cruciferous crop plants involves damage to tissues through maceration, fermentation or drying (Rabie et al., 2011; Palani et al., 2016). Glucosinolate breakdown metabolites are relevant to the properties and final use given by humans to these products (Traka, 2016). Glucosinolate metabolism has received considerable attention in recent years as a plant defense response against herbivores, for its impact on the human digestive tract and in the study of glucosinolate recycling in plant cells (Fechner et al., 2018; Gimsing and Kirkegaard, 2009; Wittstock et al., 2016; Platz et al., 2015).

Maca (*Lepidium meyenii* Walp., Brassicaceae), is an ancestral Andean root crop which is well adapted to the harsh high-altitude environment, above 4000 m, where it is usually planted. It has been the object of numerous studies related to its bioactive components with beneficial properties on fertility, cognition and energy management, among others (Yábar et al., 2011). Its traditional postharvest processing involves drying the roots in open fields over a period of up to 12 weeks during

Abbreviations: BGL (**1**), benzyl glucosinolate, glucotropaeolin; BITC (**2**), benzyl isothiocyanate; BIOC (**7**), benzyl isocyanate; BCHO (**5**), benzaldehyde; BDOH (**5a**), benzyl dialcohol; BOH (**6**), benzyl alcohol; BCN (**4**), benzyl nitrile; BNH_2 (**3**), benzylamine; BCOOH (**8**), benzoic acid; BCOOR (**8a**), benzoic acid ester; EMV, electron multiplier voltage; RH, relative humidity; RW, residual water; SIM, single ion monitoring; SPE, Solid phase extraction; SPME, Solid phase microextraction; TIC, Total ion current; VOC, Volatile organic compounds.

* Corresponding author.
E-mail address: ecosio@pucp.pe (E.G. Cosio).

https://doi.org/10.1016/j.phytochem.2020.112502
Received 22 June 2020; Received in revised form 18 August 2020; Accepted 19 August 2020
Available online 29 August 2020

which they undergo freeze-thaw cycles, intense radiative exposure and harsh mechanical manipulation. The resulting dry material is then milled into flour. Maca roots range considerably in size and their drying times vary accordingly and require sorting and collection of the dried material as the process moves along.

In a previous report (Esparza et al., 2015) we made an initial characterization of the glucosinolate and lipid hydrolytic processes which result in the final chemical profile of dried maca flour. We also provided first evidence for the exclusively postharvest origin of the benzylalkamides, macamides, present in dried roots, as a condensation product of benzylamine, a benzyl glucosinolate (**1**) breakdown metabolite, with free fatty acids generated during the drying process (Fig. 1). Later work by other groups (Chen et al., 2017; Zhang et al., 2020), has provided insights on the impact of mechanical pre-processing of the plant material and drying temperature on macamide (**9–13**) yields under laboratory conditions. However, glucosinolate hydrolysis is a fast process which, in drying tissues, is taking place continuously as tissue dehydration and disruption proceed. Our present knowledge of glucosinolate catabolism comes from bacterial, insect, mammalian and plant models (Blažević et al., 2020; Wittstock et al., 2016; Jeschke et al., 2016; Sørensen et al., 2016; Tang et al., 1972; Yábar et al., 2011). The drying of maca roots offers potentially interesting insights on the sequence of reactions, enzyme-catalyzed or spontaneous, that determine the chemical profile in root flour from a Brassicaceae.

The release and allocation of glucosinolate breakdown products during drying to various metabolic routes takes place in an environment where water potential, pH and redox status are slowly shifting and where there are progressive increases in the concentrations of free sugars and fatty acids. Prevailing conditions in the tissue may promote condensation of benzylamine and formation of bioactive amides or can lead to deamination and formation of a variety of alternative benzenoids. These two outcomes can be considered competitive and their rates depend on the existing pool of benzylamine and the mechanisms by which benzenoids can be formed from benzylamine or, possibly, directly from benzyl isothiocyanate (**2**), the major transient glucosinolate breakdown product in maca. The present report provides a detailed time-course of glucosinolate metabolites in tissues and headspace during drying under controlled conditions and proposes a sequence of competing pathways that can modulate the biochemical profile and bioactive and sensory properties of the finished flour.

2. Results

2.1. Glucosinolate hydrolytic VOC profiles

In a previous report (Esparza et al., 2015) we monitored the release of volatile glucosinolate hydrolysis products during oven drying using a headspace accumulation approach. This involved sampling with solid phase microextraction fibers (SPME) under static (no flow) headspace conditions. These conditions allowed time resolutions of over 1 h, which for the purpose of this study were unsatisfactory. We retained the relatively robust SPME sampling technique and opted instead for a flow chamber setting with access ports where we could insert temperature and relative humidity probes along with SPME fibers (Fig. S1,A and Experimental). The chamber was placed in an incubator and air flow through the chamber was regulated to ensure complete replacement of one chamber volume every 15 min. Under our temperature and air flow conditions, calculated SPME 90% equilibration times were 15 min which enabled reproducible VOC sampling during the early periods after root shredding.

Fig. 2 shows, as expected, that the 3 main hydrolysis products detected, BITC (**2**), BCN (**4**) and BIOC (**7**) display almost instantaneous rises from 0 in headspace concentration with slower drops over the next 16 h through conversion into less volatile intermediaries. The isothiocyanate (**2**) is the largest hydrolytic product with **7** and **4** amounting to about 3% of **2**, each measured as total ion current (TIC) in the mass detector. It can also be noted that all three compounds show a second, smaller, peak 24 h after start of the drying process. The most likely interpretation for this is that the very early large peak is the result of tissue damage during shredding of maca roots to generate the smaller fragments for drying. The second peak, which displays significantly slower kinetics, originates from glucosinolate hydrolysis due to destruction of tissue during drying. This process is spread over 72 h after which residual humidity in the material reaches between 2 and 8% (20–80 mg g^{-1} dry wt.).

The behavior of the other two VOCs observed, aldehyde (**5**) and alcohol (**6**), can be expected from secondary conversion products of hydrolysis. It is worth noting that while **5** displays a narrow peak at 8 h it

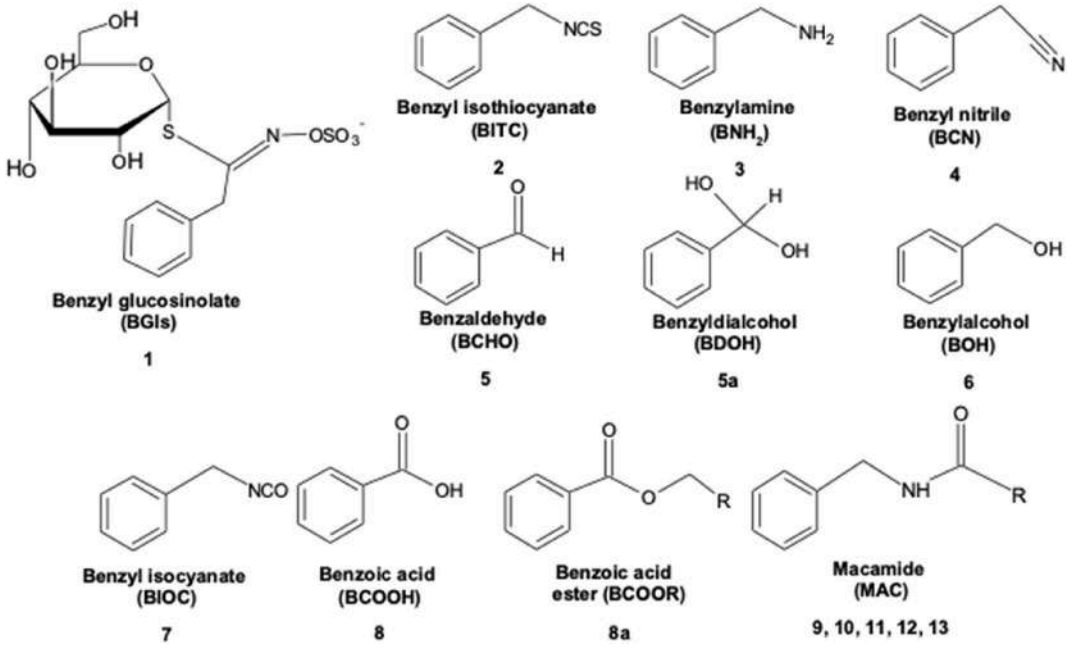

Fig. 1. Benzyl glucosinolate and hydrolytic postharvest metabolites mentioned in the text. For macamides R = palmitic acid (**9**), stearic acid (**10**), oleic acid (**11**), linoleic acid (**12**), linolenic acid (**13**).

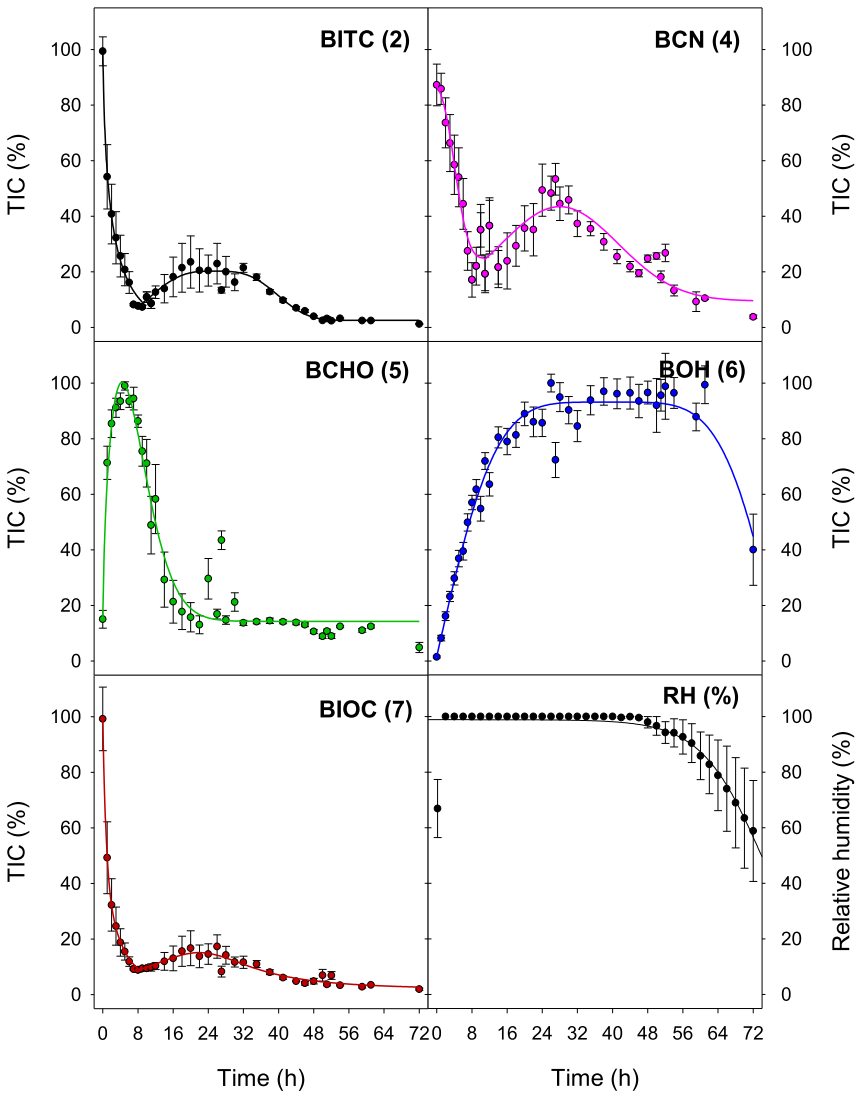

Fig. 2. Time course of major VOCs from glucosinolate hydrolysis measured by headspace SPME-GC-MS. Values are expressed as percentage of average peak total ion current (TIC) for each compound. Compounds, from top left are: benzyl isothiocyanate (BITC, **2**), benzyl nitrile (BCN, **4**), benzaldehyde (BCHO, **5**), benzyl alcohol (BOH, **6**), benzyl isocyanate (BIOC, **7**), and average relative humidity (RH) inside the chamber (N = 9). Peak TIC values (x 10^7) for the compounds were: 238.42 (**2**, 100%); 2.88 (**4**, 1.2%); 34.9 (**5**,14.6%); 28.17 (**6**, 11.8%) and 3.75 (**7**, 1.6%). Values in parenthesis after the compound number denote the relative intensity of the peak in relation to the isothiocyanate peak. RH = relative humidity in the headspace.

is detectable from very early on and, after reaching its peak, drops sharply to a lower amount, around 20% of its peak value, and remains at that level until the end of the drying period. In contrast, **6** has a much broader peak that spans from 16 to 56 h and dropping to about 40% of its peak value by the end of drying run. Maximal detector response (as Total Ion Concentration) was broadly similar for both compounds and amounted to 14.6% for **5** and 12% for **6** of the maximal response observed for the isothiocyanate (**2**). The profiles of the detected VOCs (**2, 4, 5, 6, 7**) agree with what has been reported for glucosinolate hydrolysis (Halkier and Gershenzon, 2006; Vaughn and Berhow, 2005). The time course profiles of **5** and **6**, point out to a specific generation sequence. The relatively narrow pulse of **5** in the gas phase is closely followed by the corresponding rise of **6**, which then remains stable until it tapers off as tissue desiccation increases. The amounts of **6** in the headspace only start decreasing as relative humidity in the chamber starts also dropping clearly indicating that residual water in the tissues is reaching its end point.

2.2. *Benzylamine is the primary accumulation product of glucosinolate hydrolysis in dried maca roots*

In order to correlate glucosinolate substrate concentrations with those of its volatile and semivolatile hydrolytic metabolites in the tissues during drying, we redesigned our drying chamber set up to allow for greater amounts of tissue. We modified a 70 l laboratory oven and reduced its effective volume to 35 l by setting up a plexiglass partition within the chamber. Air flow (70 l h^{-1}) entered through the bottom of the oven and moist air was eliminated through a chimney connecting the plexiglass partition with the air outlet above the oven (Fig. S1,B). The air entering the oven went through multiple outlet tubing to ensure mostly homogenous airflow from the bottom up to the exhaust chimney. A total of 640 g of shredded roots were processed in 16 steel mesh trays per experiment, the time resolution of the 72 h drying process was limited to 9 sample points for these experiments. Tissue samples were extracted directly with solvent and analyzed by GC-MS or HPLC as described in Experimental.

Fig. 3 shows the time course of glucosinolate (**1**) degradation during drying compared to those of its primary initial hydrolytic products BITC (**2**) and BCN (**4**), the main aminated product, BNH_2 (**3**), and one group of terminal accumulation products, macamides (**9**–**13**). Results are presented as molar fraction of the initial benzyl glucosinolate (**1**) amount in order to illustrate the relative flow through intermediary to final accumulation products.

Within the first few minutes one can observe a very rapid conversion of about 40% BGL (**1**) into BITC (**2**) as a result of the tissue fragmentation performed prior to the drying process. A minor amount of glucosinolate (0.05%) is converted to nitrile (**4**) in these first instants, which shows the preference under these conditions in maca for isothiocyanate

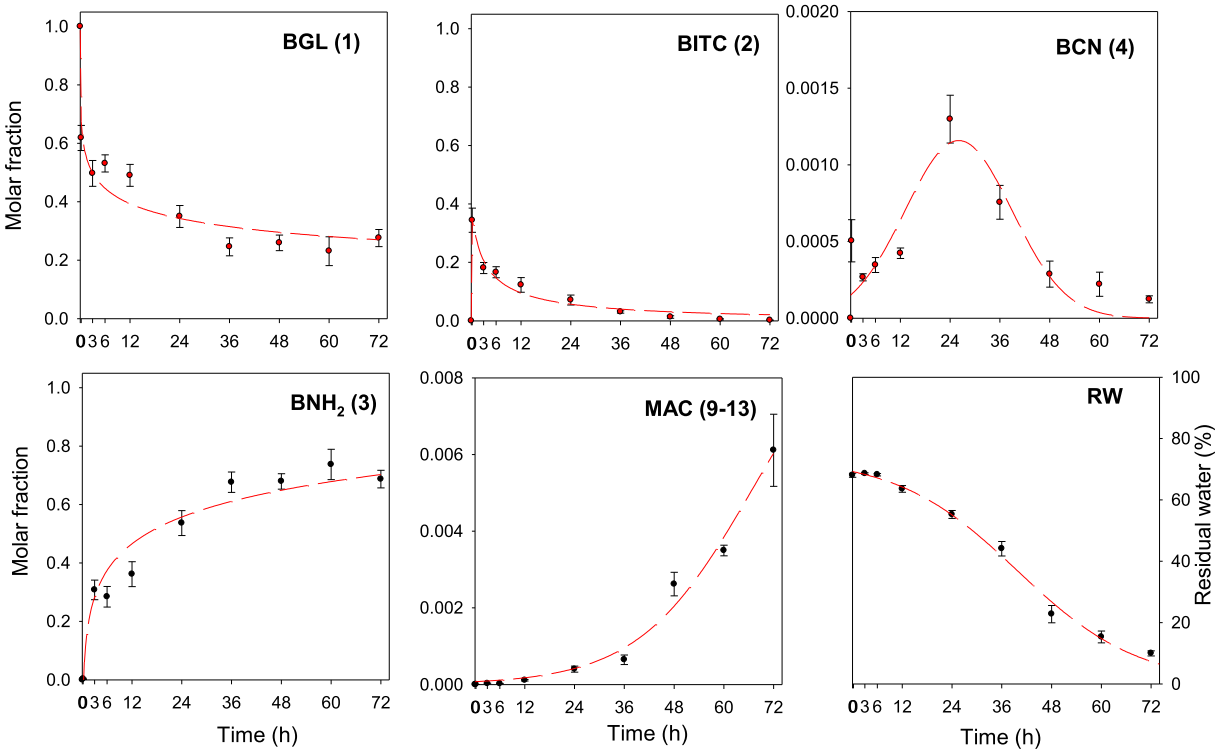

Fig. 3. Tissue concentrations during oven drying for benzyl glucosinolate (BGL) and its metabolites. Drying maca tissue was extracted in solvent and the levels of benzyl glucosinolate, its primary hydrolytic products (BITC, BCN) and two products that accumulate in the flour, benzyl amine (BNH_2) and macamides (MAC) were analyzed. RW represents residual humidity. Hydrolytic and final accumulation product patterns match those previously reported (Esparza et al., 2015), although for this study, a 72 h drying period and 35 °C constant temperature were employed. Values are expressed in molar fraction of initial glucosinolate concentration, where 1 = 36 ± 5 μmol g^{-1} dry wt. (N = 6). Nonlinear regression coefficients for the compounds were: $R^2 = 0.941$ (BGL, **1**), $R^2 = 0.971$ (BITC, **2**), $R^2 = 0.777$ (BCN, **4**), $R^2 = 0.955$ (BNH_2, **3**), $R^2 = 0.985$ (MAC, **9**–**13**) and $R^2 = 0.993$ (RW).

A

		BGL	BITC	BIOC	BCN	BNH2	MAC	BCOOR	BCHO	BCOOH	BOH
[1-0.9]	RW (%)	0.719	0.654	-0.432	0.182	-0.845	-0.923	-0.900	-0.039	-0.501	-0.485
[0.9-0.8]	BGL		0.284	-0.820	-0.335	-0.920	-0.560	-0.822	-0.760	-0.763	-0.751
[0.8-0.7]	BITC			0.045	0.151	-0.636	-0.536	-0.200	0.271	-0.070	-0.073
[0.7-0.6]	BIOC				0.614	0.625	0.286	0.697	0.390	0.263	0.255
[0.6-0.5]	BCN					0.192	-0.335	0.864	0.159	0.306	0.301
[0.5-0.4]	BNH2						0.673	0.927	0.638	0.977	0.960
[0.4-0.3]	MAC							0.899	0.084	0.651	0.630
[0.3-0.2]	BCOOR								0.426	0.878	0.873
[0.2-0.1]	BCHO									0.897	0.891
[0.1-0]	BCOOH										0.999

B

		BGL	BITC	BIOC	BCN	BNH2	MAC	BCOOR	BCHO-2	BCOOH-2	BOH-2
[1-0.9]	RW (%)	0.719	0.654	-0.432	0.182	-0.845	-0.923	-0.369	0.841	0.251	0.495
[0.9-0.8]	BGL		0.284	-0.820	-0.335	-0.920	-0.560	-0.102	0.176	-0.386	-0.134
[0.8-0.7]	BITC			0.045	0.151	-0.636	-0.536	-0.417	0.658	-0.104	0.151
[0.7-0.6]	BIOC				0.614	0.625	0.286	0.255	0.738	0.724	0.659
[0.6-0.5]	BCN					0.192	-0.335	-0.407	0.723	0.604	0.687
[0.5-0.4]	BNH2						0.673	0.201	-0.446	0.252	-0.002
[0.4-0.3]	MAC							0.584	-0.946	-0.554	-0.695
[0.3-0.2]	BCOOR-2								-0.338	-0.403	-0.230
[0.2-0.1]	BCHO-2									0.985	0.971
[0.1-0]	BCOOH-2										0.930

Fig. 4. Pearson correlation values for glucosinolate hydrolytic products. Panel A shows the correlation of metabolites for the early stage of drying, where reactions are caused by direct damage to the tissue by shredding. Panel B shows the correlation between intermediaries as a result of the late stage tissue dehydration. BCOOR-2, BCHO-2 and BCOOH-2 shown in panel B correspond to data points in Fig. 5 shown as part of the red solid line while BCOOR (**8a**), BCHO (**5**) and BCOOH (**8**) in panel A correspond to the early stage in the figure shown in solid black lines. (For interpretation of the references to colour in this figure legend, the reader is referred to the Web version of this article.)

formation over other primary hydrolytic products. Nitrile (**4**) amounts kept rising slowly over 24 h but never exceeded 0.12% of initial glucosinolate values. The rise in benzyl amine (**3**) mirrors BITC (**2**) decline with a fast rise over the first hour to about 30% of the initial glucosinolate molar amount followed by a slow increase to near 70% towards the end of the drying period. Correlation analysis supports the 1 to 3 metabolic sequence with an R^2 of −0.92 ($p < 0.05$, Fig. 4) for the patterns of the drop in benzyl glucosinolate (**1**) concentration and the corresponding rise in benzylamine (**3**). Benzylamine accounts for the largest molar percentage of final glucosinolate hydrolysis products in dried maca. Macamide formation, on the other hand, proceeds slowly, rising steeply only after 36 h but reaching a final value of only 0.6% of the initial glucosinolate molar content. Macamide accumulation displays a low positive correlation ($R^2 = 0.673$, $p = 0.033$) with that of the amine (**3**) and appears more dependent on free fatty acid availability and the advance of tissue dehydration for its formation (Esparza et al., 2015). Our results show a clear correlation of macamide formation with tissue dehydration ($R^2 = -0.923$, $p < 0.0005$) a condition which may promote condensation of fatty acids with benzylamine.

2.3. Deamination is the switching point for the formation of macamides or benzenoids

Accumulation profiles of the main deaminated benzenoid products of glucosinolate hydrolysis, benzaldehyde (BCHO, **5**), benzyl alcohol (BOH, **6**) and benzoic acid (BCOOH, **8**) are shown in Fig. 5. These measurements allowed us to distinguish between a fast hydrolytic process generated by the mechanical shredding of maca tissue to reduce its size for drying and a second, slower, process arising from tissue dehydration. We have tried to separate these two profiles through nonlinear regression. As can be observed, levels of these metabolites rise quickly just after shredding takes place (solid black lines). The initial product of this sequence is the aldehyde (**5**) which peaks at 3 h, followed by alcohol (**6**) and acid (**8**) at 6 h. Peak values for all three compounds are similar and represent between 0.2 and 0.3% of initial glucosinolate molar amounts. The second peak (solid red lines) arises from tissue dehydration and reaches a maximum at 36 h for all three compounds, after which levels drop rapidly. Peak values for this second stage show strong differences for each compound. While **5** reaches a peak of no more than 0.12% of the glucosinolate, **6** and **8** reach levels of 0.7 and 1.2% respectively. More significant are the differences in ratios between early (A) and late (B) stage peak values. While for **5** the A/B ratio is 1.5, it is 0.5 for **6** and 0.25 for **8**. This agrees with a biogenic sequence starting with **5** as the initial deamination product. The lower right panel in the figure shows the profile for benzoic acid esters (BCOOR, **8a**) with a fast early accumulation and a progressive rate reduction as the tissue dries in a manner similar to benzylamine (**3**) described in the previous section. As with **3**, benzoic esters (**8a**) display the profile of a final accumulation product, in this case as potential detoxification products of the acid (**8**). Maximal molar amounts observed in our trial were around 2.3% of initial glucosinolate values, 27 times less than amine values at the end of the drying period.

Although representing a very small fraction of total glucosinolate hydrolysis, the deaminated benzenoids combined still represent more than twice the amount of macamides formed during drying. In addition to this, benzoic acid and its esters are controlled food preservatives and higher levels in maca flour raise attention by regulators. From the observed profile sequences, deamination of **3** appears to be the source of benzaldehyde (**5**) and of the redox sequence leading to 6 and 8 with eventual accumulation of benzoic esters (**8a**).

We explored nitrogen loss in the process by monitoring ammonium ion concentration in the drying tissues. The results (Fig. 6) showed a rapid rise during the first 24 h followed by a slight drop towards the end of the drying process. Ammonium ion levels in the tissues reached

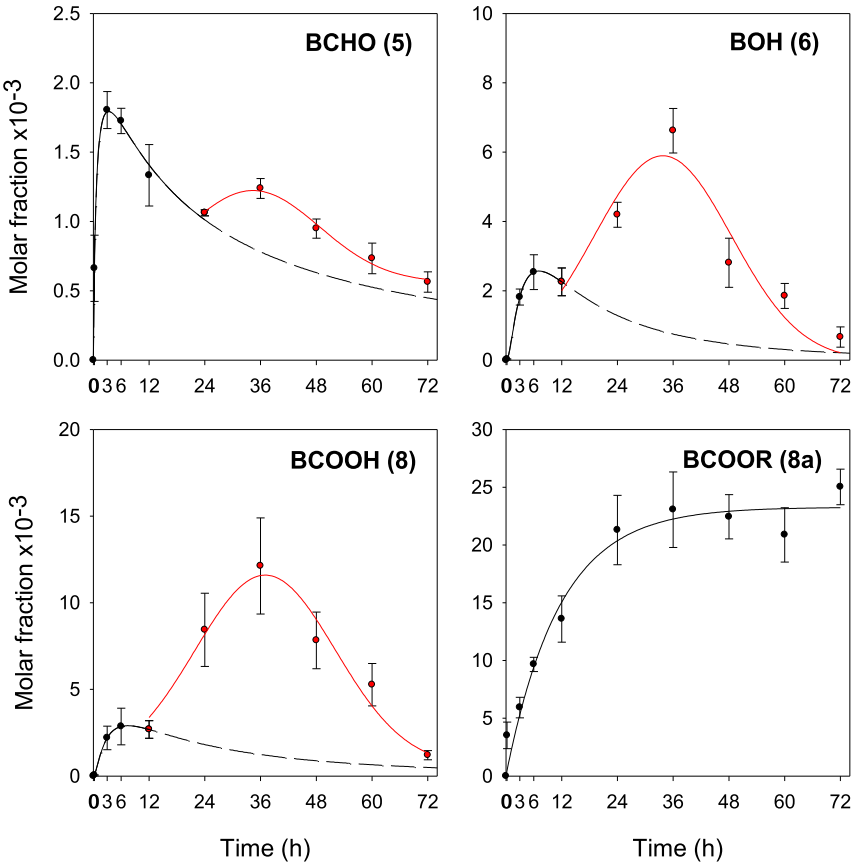

Fig. 5. Time course profiles for transient and final deaminated benzenoid products in drying maca tissues. Kinetic profiles show two stages, early "fast" kinetics (solid black lines) that take place in the initial 12 h, corresponding to damage to the tissues done by shredding to reduce size for drying and a second "slow" stage (solid red lines) that shows the dehydration of the tissues in the later part of the drying process. Data points corresponding to the initial and the late phases have been subjected to nonlinear regression separately. The nonlinear regression coefficients for the metabolites were for BCHO (**5**): $R^2 = 0.9962$ (early phase), $R^2 = 0.9880$ (late phase), for BOH (**6**): $R^2 = 0.9999$ (early), $R^2 = 0.9522$ (late), BCOOH (**8**): $R^2 = 0.9999$ (early), $R^2 = 0.9526$ (late), BCOOR (**8a**): $R^2 = 0.9677$. (For interpretation of the references to colour in this figure legend, the reader is referred to the Web version of this article.)

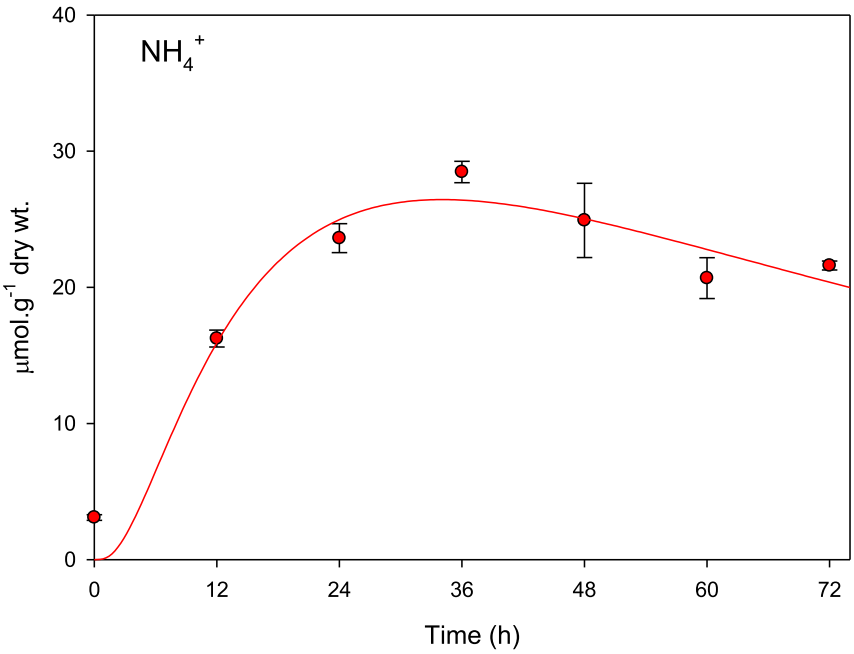

Fig. 6. Time course for the concentration of ammonium ion in maca tissues during drying. Deamination of benzyl amine and amino acids by amine oxidases are potential sources of ammonia under our short (72 h) drying conditions. Peak values of NH_4^+ are 25 µmol g^{-1} dry wt.. Total amount of deaminated benzenoids accounts for only 0.75 µmol g^{-1} dry wt. indicating other major sources of ammonium in the process. Curve adjusted by nonlinear regression ($R^2 = 0.9472$).

maximal concentration between 24 and 36 h of drying time, coinciding with the benzenoid peak. With peak values around 25 µmol g^{-1} dry wt., ammonium represents 100% of benzylamine nitrogen molar amount, a considerable excess over the estimated 3% of benzenoids that would have actually arisen from deamination of glucosinolate hydrolytic products under our experimental conditions. Ammonium release has to be accounted for from other nitrogenated sources during drying.

3. Discussion

3.1. Benzylamine pool arises from isothiocyanate hydrolysis while tissues are still in a hydrated stage

Fig. 7 summarizes a proposed metabolic scheme for the drying process based on the findings presented here. We have divided it in steps, A through F, that group metabolic reactions taking place at different stages

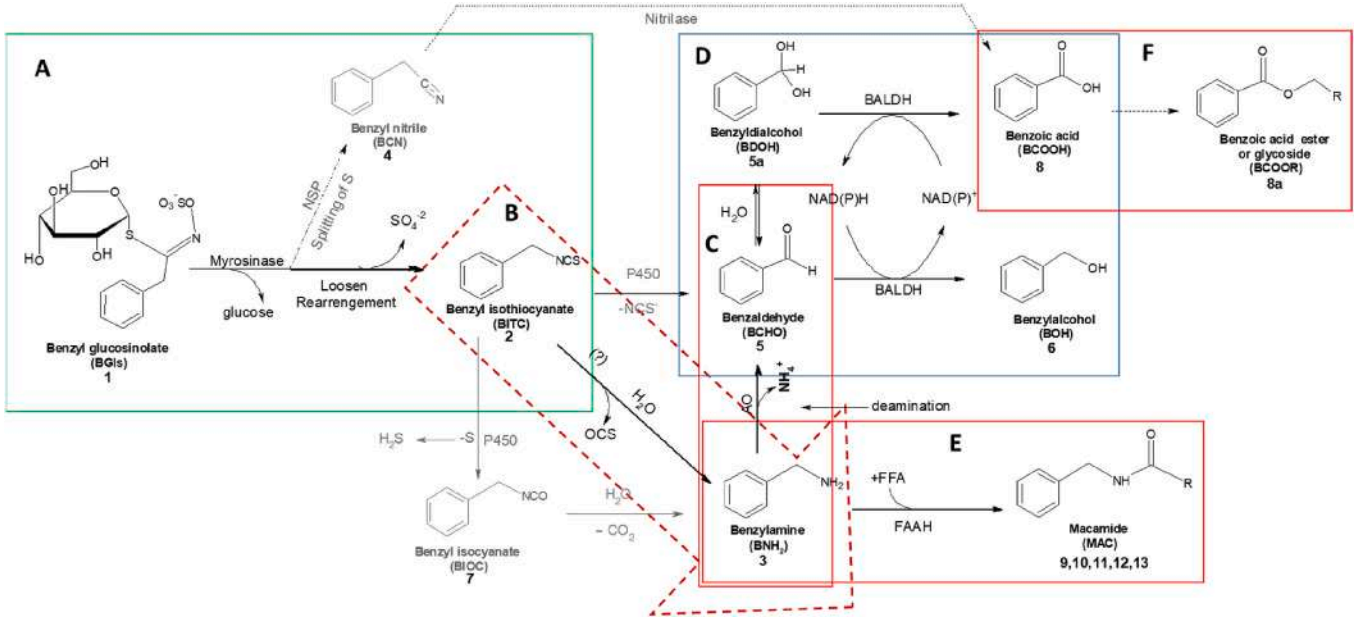

Fig. 7. Proposed scheme for reactions taking place during the maca drying. The sequence is based on the main hydrolytic metabolites observed during the drying process. Step A describes reactions generating the initial hydrolysis products and including BITC (**2**), BCN (**4**) and BIOC (**7**). Step B is the formation of BNH_2 (**3**), the main accumulation product, from BITC (**2**). Step C describes deamination of BNH_2 (**3**) to generate various deaminated benzenoids. Step D corresponds to the disproportionation reactions leading to pools of BCHO (**5**), BOH (**6**) and BCOOH (**8**) through the action of an aldehyde dehydrogenase. Step E is the condensation of BNH_2 (**3**) with free fatty acids to produce macamides (MAC **9**–**13**) and step F corresponds to esterification or glycosylation of BCOOH (**8**) as a detoxification mechanism. Numbers correspond to those in Fig. 1. Dark lines show favored reactions according to our results. Compounds in light gray are minor transient products.

of tissue hydration and levels of oxidation.

Steps A and B, as seen in section 2.2, point out to strong evidence for a BGL (**1**)-BITC (**2**)-BNH_2 (**3**) sequence for glucosinolate hydrolysis during drying. This observation coincides with previous reports on the mechanism for glucosinolate thermal degradation (De Nicola et al., 2012). Thermal hydrolysis of **2** in aqueous solution can take place through the attack of a water molecule that incorporates an OH into the central electrophilic carbon of the isothiocyanate to form a benzoylcarbamothionic O-acid with release of carbonyl sulfide to form benzylamine (**3**) (Fig. S2). Although the mechanism, as described, suggests a spontaneous reaction, it by no means rules out enzyme involvement in our particular conditions with active site residues generating the OH^- nucleophile. This reaction is rapid and takes place mostly during the initial hours of the drying process, when the tissues are still highly hydrated. It is noteworthy that the amine (**3**) is the main product observed in maca. There are few reports on glucosinolate-like free amines accumulating at this level (Agerbirk and Olsen, 2012). Blažević et al. (2020) have recently reported such an occurrence but in lesser proportions through conjugation of indol-3-ylmethyl isothiocyanate with glutathione and subsequent hydrolysis to form indol-3-ylmethyl amine.

After 24 h the rate of accumulation drops and the concentration of **3** in the tissues rises only very slowly due to limited rates of isothiocyanate (**2**) hydrolysis in the now drier environment. Once the amine is formed, it appears relatively stable and accumulates under increasingly dehydrated conditions. Limited losses from the amine pool are mediated by two competing reactions. One is deamination to benzaldehyde (**5**) (step C) through the action of amine oxidases present in the tissue and followed by a disproportionation reaction (step D) as explained in the next section to form the corresponding alcohol (**6**) or carboxylic acid (**8**). The alternative, step E, is condensation of the amine (**3**) with free fatty acids arising from the slow hydrolysis of storage triglycerides and membrane lipids to produce amides (**9**–**13**). This reaction appears to be favored in dehydrating tissue as explained by the slow accumulation kinetics observed for the macamides. During the initial phases of drying, when tissue hydration is high and free fatty acid concentration is still low is when peaks of the deaminated benzenoids (**5**, **6**, **8**) can be observed. As residual humidity in the tissues drops, condensation with fatty acids to form amides increases ($R^2 = 0.92$) and also the formation of esters and glycosides of **8** becomes important ($R^2 = 0.9$) (step F). These reactions appear to be favored in the presence of low residual humidity in the tissues.

3.2. Are maca benzenoids generated by an aldehyde dehydrogenase acting in a bio-Canizzaro reaction pattern?

As pointed out in section 2.3, peak concentrations of deaminated benzenoids display sequentially higher values (in molar fraction of initial glucosinolate); 0.12% (BCHO, **5**), 0.7% (BOH, **6**), 1.2% (BCOOH, **8**) and 2.1% (BCOOR, **8a**). The first three are transient, peaking at 36 h, while benzoic esters (**8a**) accumulate during drying. Conjugates and esters are common detoxification products in dicot vacuoles (Matile, 1990). Published reports indicate that fee benzoic acid is eliminated rapidly through these procedures in plants (Chrikishvili et al., 2006) The release of benzoic acid from glucosinolate catabolism during tissue drying very likely triggers reactions leading to the formation of these moieties and this process can provide the metabolic "pull" for oxidation of **5** into **8**. On the other hand, the temporal and molar ratio relationships between **5**, **6** and **8** suggest an interlinked process that could be explained invoking an asymmetric Canizzaro-type reaction where the aldehyde is substrate and alcohol and acid are products. Correlation analysis (Fig. 4) shows high values between **5** and **8** ($R^2 = 0.985$, $p < 0.05$) and between **5** and **6** ($R^2 = 0.971$, $p < 0.05$). This process has been proposed for a number of prokaryotic and eukaryotic aldehyde dehydrogenases (Wuensch et al., 2013) and provides adequate explanation for the observed behavior, requiring only one enzyme, as opposed to needing an additional aldehyde oxidase (Ibdah et al., 2009) and being essentially redox neutral (Fig. 8). According to this model, two half-reactions are catalyzed by the enzyme. The aldehyde in aqueous solution is in equilibrium with its diol form (**5a**) and provides substrate for both. The oxidative half-reaction leads from the diol (**5a**) to benzoic acid (**8**) and the reductive half-reaction converts aldehyde (**5**) into benzyl alcohol (**6**). This sequence, as described, should lead to the accumulation of **8** and **6**, however neither is a final accumulation product in our experiments. Benzoic acid removal takes place through conversion into esters (**8a**) (Fig. 7 step F), a process that explains why it does not accumulate. The lack of accumulation of (**6**), which appears as a transient product peaking in the tissue at 36 h requires a more elaborate explanation. Two possibilities could explain this, the concentration of **6** in the gas phase, as observed using SPME-GC-MS (Fig. 2) starts peaking only at 8 h reaching a signal value 14% of that of isothiocyanate (**2**) and stays at maximal values almost throughout the drying process. This is under conditions of constant airflow through the chamber which constantly removes the alcohol from the gas phase. Benzaldehyde (BCHO, **5**) peaks very early in the gas phase, at 8 h, with signal values about 12% of the isothiocyanate peak, and drops quickly so that by 24 h levels are close to only 2% of the peak isothiocyanate signal, and remain like that until the end of the process. We speculate that conversion of **5** into **6** as shown in Fig. 8 results in removal of this product from the tissue through evaporation and gas transport as shown by the VOC kinetics. Boiling points of 178 °C (**5**), 205 °C (**6**) and 250 °C (**8**) suggest the potential for gas phase removal of both (**5**) and (**6**) but (**5**) is also being processed enzymatically into alcohol and acid which also explains its transient appearance as a VOC. A second factor that could explain the removal of **6** is esterification with **8** or another short chain free acid. This would produce benzyl benzoate, a product whose detection proved inconsistent in these experiments, or benzyl acetate, which we have also observed infrequently in analyses of the samples, which lends more weight to the gas phase removal explanation.

3.3. Conclusions

The biochemistry of traditional maca root postharvest drying is a slow and complex process, spread over 6–8 weeks until complete. This study used 72 h low-temperature oven drying conditions under air flow to explore the factors that influence the final composition of glucosinolate breakdown products in the dry product. Following the profile of hydrolytic metabolites on a molar fraction basis of initial glucosinolate allowed us to account for 99% of all benzyl moieties present at the end of the drying process. The results show clearly that the primary accumulation product of benzyl glucosinolate after tissue drying is benzyl amine which accounts for over 94% of hydrolyzed substrate. In dehydrated tissue the amine is very stable and other products derived from its metabolism, such as macamides or deaminated benzenoids, account for

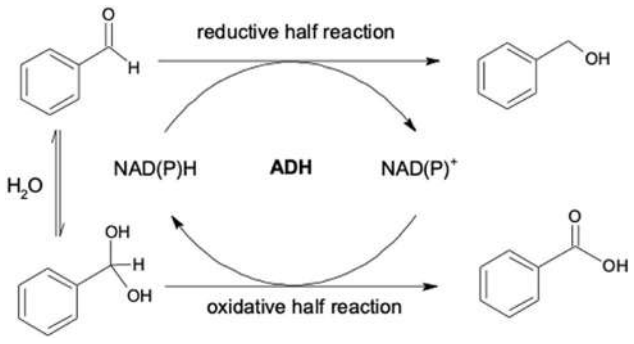

Fig. 8. Reaction scheme for the formation of BOH (**6**) and BCOOH (**8**) from reactive benzaldehyde through a Cannizzaro type reaction, catalyzed by a benzaldehyde dehydrogenase (based on Wuensch et al., 2013). The proposed scheme would require only one enzymatic activity for both the oxidative and reductive half-reactions.

less than 5% of starting material. The observed results allow to speculate that the rate of dehydration modulates the degree of benzyl amine conversion into other products and, more relevant, whether these condense with fatty acids to form macamides or are deaminated and accumulate as benzoic acid esters. It has been speculated previously (Esparza et al., 2015) that macamide formation could be optimized by playing with the molar ratio of amine to fatty acid, which is usually 10:1. This study suggests that the determinant factor is the rate of dehydration. Amide formation seems to be favored once hydration of the tissue is significantly reduced. A slow rate of dehydration with tissue damage favors the deamination of benzylamine and the formation of aldehyde, alcohol and acid benzenoid moieties through the action of amine oxidases and an aldehyde dehydrogenase catalyzing a disproportionation in a Canizzaro-like reaction. The prevailing redox and hydration conditions in the tissue will favor then the accumulation of benzyl alcohol and benzoic acid. The esterification of the acid provides a metabolic pull in its direction while benzyl alcohol goes into the gas phase and is eliminated in greater part both in oven and field conditions.

4. Experimental

4.1. General procedures and instrumentation

Structural characterization of synthetic amides was performed using a Bruker 500 UltraShield NMR (Karlsruhe, Germany), a PerkinElmer series 1600 FT-IR spectrometer (Waltham, MA) and a Thermo Spectronic Genesys 6 (Rochester, NY) UV/Vis spectrophotometer. Data collection for environmental variables for oven drying experiments used OM-62 units from Omega Engineering (Stamford, CN), for ambient laboratory conditions and a XR5 SE system from Pace Scientific (Mooresville, NC) equipped with a TRH-100 temperature and humidity sensor for inside the drying oven. Statistical treatment and nonlinear regression analyses were performed using SigmaPlot 11 for Windows (Systat Software).

4.2. Chemicals

Benzyl glucosinolate (**1**) was obtained from Calbiochem/Merck Biosciences (San Diego, CA). Benzyl isothiocyanate (**2**), benzyl nitrile (**4**), benzyl alcohol (**5**), benzaldehyde (**6**), benzyl isocyanate (**7**), fatty acids and reagents for amide synthesis were obtained from Sigma–Aldrich (St. Louis, MO). Benzoic acid (**8**) and benzylamine (**3**) were from Merck (Darmstadt, Germany). The benzylamides of palmitic (MAC16, **9**), stearic (MAC18, **10**), oleic (MAC18-1, **11**), linoleic (MAC18-2, **12**) and linolenic (MAC18-3, **13**) acids were synthesized in our laboratory for use as standards according to Esparza et al. (2015). All other solvents and reagents were analytical or HPLC grade.

4.3. Plant material

Fresh yellow maca roots were obtained from a local market and originated from the Junín region in central Peru. Oven drying tests in the laboratory were carried out using maca roots of a uniform size, approximately 3 cm in diameter. These were washed with distilled H_2O, pat-dried with filter paper and shredded manually into 2 mm-strips using a kitchen stainless steel vegetable shredder.

4.4. Oven drying experiments

Six hundred and 40 g of shredded fresh maca roots were placed in sixteen 100 cm^2 stainless steel mesh trays (40 g fresh wt./tray) and placed in a 70 l oven at 35 °C. Moist air was pumped into the oven through an activated charcoal trap and a chamber with distilled water, both at lab temperature (22 °C). Duplicate random samples were taken at 3, 6, 12, 24, 36, 48, 60 and 72 h, and mixed gently to homogenize them and separated into duplicate samples, weighed and stored in aluminum foil pouches in liquid N_2 until analyzed by HPLC and GC–MS. The time zero sample was shredded directly into liquid N_2 for storage. Three independent drying experiments were carried out at different times and the results presented here are average values (N = 6).

4.5. Extraction of plant material

Shredded maca samples (1 g), frozen in liquid N_2, were placed in polypropylene centrifuge tubes (15 ml) containing H_2O–MeOH (10 ml, 30:70, v/v) preheated to 70 °C. The tubes were flushed with N_2 gas, closed, placed in a heated water bath at 70 °C for 10 min and then sonicated for 30 min. They were then centrifuged at 10000×*g* for 15 min. The supernatant was vacuum filtered through Whatman GF/A filters and the filtrate collected in glass culture tubes (50 ml) with Teflon-lined caps. The pellet was re-extracted for 10 min and the filtered supernatants were pooled. Samples were stored under N_2 at −20 °C until analyzed.

4.6. Analysis of amides and free fatty acids

Macamides (**9**–**13**) and free unsaturated fatty acids were analyzed using a modification of previously reported methods (Esparza et al., 2015; Ganzera et al., 2002; McCollom et al., 2005). Samples were dissolved in H_2O–MeOH (7 ml, 50:50, v/v) and loaded onto a Merck Lichrolut RP-18 (500 mg) reversed phase SPE column. The columns were washed with 5 ml H_2O–MeOH (50:50, v/v) and eluted with 2 ml MeOH. The eluate was analyzed in an Agilent Infinity 1290 UPLC quaternary pump system coupled to a diode array detector in series with an Agilent 6120 single quadrupole mass detector using atmospheric pressure chemical ionization (APCI). Instrument conditions were: drying gas temperature 250 °C, vaporization temperature 400 °C, drying gas flow 9.0 l min^{-1}, nebulization pressure 25 psi, capillary voltage (positive) 4000 V, (negative) 4000 V, Corona (positive) 4 μA, (negative) 4 μA. Signals in full scan 80–550 m/z, APCI mode, (50% time each polarity), signals in SIM mode (see Table S1 supplementary material).

Samples (10 μl) were injected into a Merck LiChrospher 100 RP-18 column, 150 mm × 4.6 mm i. d. (5 μm). The column heater was set at 40 °C and flow rate was 1 ml min^{-1}. The solvent program is shown in Table S2. The results present total macamides as a sum of compounds **9**–**13**.

4.7. Analysis of benzylamine and free amino acids

Amines were analyzed by derivatization with *o*-phthaldialdehyde (OPA, Sigma, St. Louis, MO) followed by reversed phase HPLC. The reagent contained OPA (27 mg) in MeOH (0.5 ml) diluted with sodium borate buffer (5 ml) and 2-mercaptoethanol (25 μL). Each pooled MeOH extract (180 μl) was diluted with 0.4 M Na borate buffer (25 μl, pH 9.5) and 20 μl of tyramine 0.1 mg ml^{-1} was used as internal standard, before adding OPA reagent (25 μl). The mix was vortexed for 1 min, centrifuged for 2 min at room temperature and 10 μl were injected for HPLC analysis.

The HPLC instrument used was an Agilent 1260 Infinity II. The column used was a Merck LiChrospher 100 RP-18, 125 mm × 4.6 mm i. d. (5 μm). Oven temperature was kept at 30 °C and detection was performed at 340 nm. The solvent system consisted of MeOH (solvent A) and 20 mM NaOAc buffer, pH 6.0 (solvent B). The program consisted of a 9 min gradient from 40% to 100% A and 4 min at 100% A (Esparza et al., 2015; Simons and Johnson, 1978).

4.8. Analysis of glucosinolates

Benzylglucosinolate (**1**) was analyzed as its desulfated product with slight modification from the literature (Brown et al., 2003; Møldrup et al., 2011). One ml of the pooled hypocotyl extracts, obtained as in 4.5, was diluted to MeOH–H_2O (50:50, v/v) by addition of 0.5 ml of water. A

1.5 ml aliquot was applied into conditioned Agilent Bond Elut-SAX SPE columns (500 mg). The latter were washed sequentially with MeOH–H_2O (5 ml, 70:30, v/v) and then conditioned with 0.02 M MES buffer (Sigma, St. Louis, MO) (1 ml, pH 5.2) after which 150 μl (150 units) of sulfatase (H-1, *Helix pomatia*, Sigma, St. Louis, MO) was added and the columns were incubated overnight at room temperature. The following day desulfoglucosinolates were sequentially eluted with MeOH–H_2O (800 μl, 70:30, v/v) and H_2O (800 μl). Both eluates were pooled in 2 ml autosampler vials and used directly for analysis. HPLC analysis was performed using a Merck LiChrospher 100 RP-18, 250 mm × 4.6 mm i. d. (5 μm) column, column heater temperature 30 °C and a 1 ml min^{-1} flow rate. Samples (20 μl) were injected and elution was monitored at 230 nm. The gradient program used CH_3CN (solvent A) and H_2O (solvent B) and was as follows: 6 min from 2% A to 5% A, 2 min 5% A to 7% A, 10 min 7% A to 21% A, 5 min 21% A to 29% A, 2 min 29% A to 100% A and 2 min at 100% A (Brown et al., 2003).

4.9. VOC analysis

Headspace solid phase micro-extraction (HS-SPME) of volatiles was performed using fused silica fibers coated with a 30 μm layer of DVB/Carb/PDMS (divinylbenzene/carboxen/polydimethylsiloxane) (Supelco, Bellefonte, PA). The fibers were conditioned following the manufacturer's instructions by exposure in the GC injection port at 270 °C for 30 min. For the analysis, shredded maca (10 g) was placed in a closed, 600 ml cylindrical glass chamber with 6 glass ports with screw cap: two for air flux inlet and outlet, three for volatile sampling with PTFE septa and one for a temperature and humidity sensor (Figure S1A). The chamber was placed in an oven at 35 °C, constant air flow (40 ml min^{-1}) was provided by an aquarium pump and previously filtered with an activated carbon filter. SPME fibers were introduced through the septa to expose them to the headspace within. SPME fibers were exposed to the headspace for 15 min. Samples were taken at different times intervals (from 0 to 8 h, every hour, from 8 to 72 h, every 3 h) for analysis by headspace GC–MS analysis.

After exposure, the fibers were inserted into the injection port of the GC for analysis and exposed for 8 min. GC–MS analysis was performed using an Agilent 7890 B GC coupled to a 5977 single quadrupole MSD. The GC was equipped with a VF-23 ms column (30 m × 0.25 mm, 0.25 μm film thickness). Injector temperature was set at 250 °C, splitless, and He carrier gas flow rate was 1 ml min^{-1}. The oven temperature was initially held at 45 °C for 4 min, and then raised to 190 °C at 15 °C min^{-1}, then to 240 °C at 30 °C min^{-1} and finally held for 2 min at 240 °C. Electron ionization was set at 70 eV. Identification of the compounds was performed by the use of pure standards, retention indices and by mass spectral analysis used AMDIS 32 (version 2.69, NIST), the NIST Mass Spectral Search Program and the NIST 2011 mass spectral library.

4.10. Analysis of glucosinolate hydrolytic products

Shredded maca samples (1 g) were extracted with 20 ml of CH_2Cl_2 in an ultrasonic bath (Branson 5800, Danbury, CT) set at 30 °C and 40 Hz for 1 h. The supernatant was filtered through a sodium sulfate column with a GF/A filter to a 50 ml glass tube.

For the analysis of the lower abundance compounds (**4**,**5**,**6**,**7**), extracts were analyzed by GC-MS in an Agilent 7890 B equipped with a multimode injector (MMI) in solvent-vent mode. Samples (25 μl) were injected and the injector was held at −5 °C with pressurized liquid nitrogen for 3.3 min to vent excess solvent, then taken to 250 °C at 600 °C min^{-1}, and held at 250 °C for 2 min. Separation was performed in a VF-23 ms (30 m × 0.25 mm, 0.25 μm) column and the eluate analyzed in an Agilent 5977 quadrupole mass detector as described in 3.9. The temperature program started at 45 °C, and taken to 190 °C at 15 °C min^{-1}, then to 240 °C at 30 °C min^{-1}, and held for 2 min at 240 °C. The analysis of BITC (**2**), a major primary hydrolytic product, required only the injection of 1 μl, of extract using a split ratio of 20:1 and injector temperature 250 °C. All other conditions remained unchanged.

4.11. Benzoic acid extraction and analysis

Ten ml of acidified CH_2Cl_2 (0.1% HCl) were used to extract the equivalent to 0.5 g dry weight of maca in 10 ml glass tubes with PTFE liner screwcaps. Samples were vortexed for 30 s and then sonicated for 1 h at 30 °C. Extracts were dried through a sodium sulfate column, collected in 12 ml glass vials, and stored under nitrogen at −20 °C until analysis.

For GC analysis, benzoic acid (**8**) was derivatized with MSTFA as follows: 2 ml of CH_2Cl_2 extract were dried in a centrifugal evaporator (Concentrator Plus, Eppendorf) in alcoholic vacuum mode at 30 °C for 20 min, redissolved in 250 μl of CH_2Cl_2, transferred to a 250 μl GC vial insert and dried in the concentrator at 45 °C for 15 min. MSTFA was added (20 μl) and heated to 60 °C for 30 min (Senger et al., 2005). After cooling for 10 min, 80 μl of methylene chloride was added. One μl of sample was injected into an Agilent 7890 A GC-FID, equipped with a DB-5 column (30 m × 0.25 mm, 0.25 μm). Injector temperature was 250 °C, split 10:1, gas flow 1 ml min^{-1}. The temperature program started at 50 °C for 4 min, rose to 180 °C at 25 °C min^{-1}, then to 250 °C at 10 °C min^{-1}, and finally to 280 °C at 30 °C min^{-1} and held for 5 min.

4.12. Hydrolysis of benzoic acid esters

Three ml of 70% maca MeOH extract (from 4.5) were taken to 50% MeOH, 1 N HCl (800 μl of water and 400 μl of concentrated HCl were added to the 3 ml of extract) and heated to 100 °C for 1 h in a dark vial. After the mix had cooled, 2 ml of methylene chloride were added and vortexed for 30 s and then centrifuged at 100×*g* for 10 min. The organic phase was collected, dried with sodium sulfate, vortexed for 10 s, centrifuged at 100×*g* for 10 min, and 1.5 ml of supernatant were transferred to a 2 ml vial and concentrated to 100 μl in a Concentrator plus (Eppendorf) in vacuum-alcoholic mode for 20 min, and transferred to a GC vial insert, dried and processed as in the previous section.

4.13. Ammonia analysis

One hundred μl of 70% maca MeOH extract (from 4.5) were taken for derivatization with diethyl ethoxymethylene malonate (DEEMM) adding 175 μl of sodium borate buffer (1 M, pH 9.4), 75 μl of methanol and 3 μl of DEEMM. Samples were sonicated for 45 min at 30 °C, placed in a heating block for 2 h at 70 °C, centrifuged at 20000×*g* for 5 min and the supernatant used for analysis. An Agilent 1260 Infinity II HPLC quaternary pump system with diode array detector was used, with a Merck LiChrospher 100 RP-18 (5 μm) LiChroCART 250-4 RP-18 (250 mm × 4 mm, 5 μm). Flow rate was 1 ml min^{-1} and column heater was set to 40 °C. Samples (10 μl) were injected and elution was monitored at 280 nm. The solvent system consisted of acetonitrile (solvent A) and 20 mM NaOAc buffer, pH 4.2 (solvent B). The solvent gradient was 2 min from 20 to 30% A, hold 3 min at 30% A, 5 min from 30% to 50% A, and hold 2 min at 50% (Gómez-Alonso et al., 2007; Redruello et al., 2013).

Declaration of competing interest

The authors declare that they have no known competing financial interests or personal relationships that could have appeared to influence the work reported in this paper.

Acknowledgments

We wish to acknowledge financial support from the PROGRAMA NACIONAL DE INNOVACION AGRARIA – PNIA (023-2016-PNIA). We also thank Ecoandino S.A.C. for plant and processed material. E.E. received support from PNIA for an internship at the University of Copenhagen (KU). We thank Drs. Fernando Geu-Flores and Niels Agerbirk of KU for discussions and ideas.

Appendix A. Supplementary data

Supplementary data to this article can be found online at https://doi.org/10.1016/j.phytochem.2020.112502.

References

Agerbirk, N., Olsen, C.E., 2012. Glucosinolate structures in evolution. Phytochemistry 77, 16–45. https://doi.org/10.1016/j.phytochem.2012.02.005.

Blažević, I., Montaut, S., Burčul, F., Olsen, C.E., Burow, M., Rollin, P., Agerbirk, N., 2020. Glucosinolate structural diversity, identification, chemical synthesis and metabolism in plants. Phytochemistry 169, 1. https://doi.org/10.1016/j.phytochem.2019.112100.

Brown, P.D., Tokuhisa, J.G., Reichelt, M., Gershenzon, J., 2003. Variation of glucosinolate accumulation among different organs and developmental stages of *Arabidopsis thaliana*. Phytochemistry 62, 471–481. https://doi.org/10.1016/S0031-9422(02)00549-6.

Chen, J.J., Zhao, Q.S., Liu, Y.L., Gong, P.F., Cao, L., Wang, X.D., Zhao, B., 2017. Macamides present in the commercial maca (*Lepidium meyenii*) products and the macamide biosynthesis affected by postharvest conditions. Int. J. Food Prop. 20, 3112–3123. https://doi.org/10.1080/10942912.2016.1274905.

Chrikishvili, D., Sadunishvili, T., Zaalishvili, G., 2006. Benzoic acid transformation via conjugation with peptides and final fate of conjugates in higher plants. Ecotoxicol. Environ. Saf. 64, 390–399. http://doi:10.1016/j.ecoenv.2005.04.009.

De Nicola, G.R., Montaut, S., Rollin, P., Nyegue, M., Menut, C., Iori, R., Tatibouët, A., 2012. Stability of benzylic-type isothiocyanates in hydrodistillation-mimicking conditions. J. Agric. Food Chem. 61, 137–142. https://doi.org/10.1021/jf3041534.

Esparza, E., Hadzich, A., Kofer, W., Mithöfer, A., Cosio, E.G., 2015. Bioactive Maca (*Lepidium meyenii*) alkamides are a result of traditional Andean postharvest drying practices. Phytochemistry 116, 138–148. https://doi.org/10.1016/j.phytochem.2015.02.030.

Fechner, J., Kaufmann, M., Herz, C., Eisenschmidt, D., Lamy, E., Kroh, L.W., Hanschen, F. S., 2018. The major glucosinolate hydrolysis product in rocket (*Eruca sativa* L.), sativin, is 1,3-thiazepane-2-thione: elucidation of structure, bioactivity, and stability compared to other rocket isothiocyanates. Food Chem. 261, 57–65. https://doi.org/10.1016/j.foodchem.2018.04.023.

Ganzera, M., Zhao, J., Muhammad, I., Khan, I.A., 2002. Chemical profiling and standardization of *Lepidium meyenii* (Maca) by reversed phase high performance liquid chromatography. Chem. Pharm. Bull. 50, 988–991. https://doi.org/10.1248/cpb.50.988.

Gimsing, A.L., Kirkegaard, J.A., 2009. Glucosinolates and biofumigation: fate of glucosinolates and their hydrolysis products in soil. Phytochemistry Rev. 8, 299–310. https://doi.org/10.1007/s11101-008-9105-5.

Gómez-Alonso, S., Hermosín-Gutiérrez, I., García-Romero, E., 2007. Simultaneous HPLC analysis of biogenic amines, amino acids, and ammonium ion as aminoenone derivatives in wine and beer samples. J. Agric. Food Chem. 55, 608–613. https://doi.org/10.1021/jf062820m.

Halkier, B.A., Gershenzon, J., 2006. Biology and biochemistry of glucosinolates. Annu. Rev. Plant Biol. 57, 303–333. https://doi.org/10.1146/annurev.arplant.57.032905.105228.

Ibdah, M., Chen, Y.T., Wilkerson, C.G., Pichersky, E., 2009. An aldehyde oxidase in developing seeds of *Arabidopsis* converts benzaldehyde to benzoic acid. Plant Physiol. 150, 416–423. https://doi.org/10.1104/pp.109.135848.

Jeschke, V., Gershenzon, J., Vassao, D.G., 2016. Insect detoxification of glucosinolates and their hydrolysis products. Adv. Bot. Res. 80, 199–245. https://doi.org/10.1016/bs.abr.2016.06.003.

McCollom, M.M., Villinski, J.R., McPhail, K.L., Craker, L.E., Gafner, S., 2005. Analysis of macamides in samples of Maca (*Lepidium meyenii*) by HPLC-UV-MS/MS. Phytochem. Anal. 16, 463–469. https://doi.org/10.1002/pca.871.

Matile, P., 1990. The toxic compartment of plant cells. In: Progress in Plant Cellular and Molecular Biology Current Plant Science and Biotechnology in Agriculture, pp. 557–566. https://doi:10.1007/978-94-009-2103-0_84.

Møldrup, M.E., Geu-Flores, F., Olsen, C.E., Halkier, B.A., 2011. Modulation of sulfur metabolism enables efficient glucosinolate engineering. BMC Biotechnol. 11, 12. https://doi.org/10.1186/1472-6750-11-12.

Palani, K., Harbaum-Piayda, B., Meske, D., Keppler, J.K., Bockelmann, W., Heller, K.J., Schwarz, K., 2016. Influence of fermentation on glucosinolates and glucobrassicin degradation products in sauerkraut. Food Chem. 190, 755–762. https://doi.org/10.1016/j.foodchem.2015.06.012.

Platz, S., Kühn, C., Schiess, S., Schreiner, M., Kemper, M., Pivovarova, O., Pfeiffer, A.F. H., Rohn, S., 2015. Bioavailability and metabolism of benzyl glucosinolate in humans consuming Indian cress (*Tropaeolum majus* L.). Mol. Nutr. Food Res. 60, 652–660. https://doi.org/10.1002/mnfr.201500633.

Rabie, M.A., Siliha, H., el-Saidy, S., el-Badawy, A.A., Malcata, F.X., 2011. Reduced biogenic amine contents in sauerkraut via addition of selected lactic acid bacteria. Food Chem. 129, 1778–1782. https://doi.org/10.1016/j.foodchem.2011.05.10600.

Redruello, B., Ladero, V., Cuesta, I., Álvarez-Buylla, J.R., Martín, M.C., Fernández, M., Alvarez, M.A., 2013. A fast, reliable, ultra high performance liquid chromatography method for the simultaneous determination of amino acids, biogenic amines and ammonium ions in cheese, using diethyl ethoxymethylenemalonate as a derivatising agent. Food Chem. 139, 1029–1035. https://doi.org/10.1016/j.foodchem.2013.01.071.

Senger, T., Wichard, T., Kunze, S., Göbel, C., Lerchl, J., Pohnert, G., Feussner, I., 2005. A multifunctional lipoxygenase with fatty acid hydroperoxide cleaving activity from the moss *Physcomitrella patens*. J. Biol. Chem. 280, 7588–7596. https://doi.org/10.1074/jbc.M411738200.

Simons, S.S., Johnson, D.F., 1978. Reaction of *o*-phthalaldehyde and thiols with primary amines: fluorescence properties of 1-alkyl(and aryl)thio-2-alkylisoindoles. Anal. Biochem. 90, 705–725. https://doi.org/10.1016/0003-2697(78)90163-X12100.

Sørensen, J.C., Frandsen, H.B., Jensen, S.K., Kristensen, N.B., Sørensen, S., Sørensen, H., 2016. Bioavailability and *in vivo* metabolism of intact glucosinolates. Journal of Functional Foods 24, 450–460. https://doi.org/10.1016/j.jff.2016.04.023.

Traka, M.H., 2016. Health benefits of glucosinolates. Adv. Bot. Res. 80, 247–279. https://doi.org/10.1016/bs.abr.2016.06.004.

Tang, C.S., Bhothipaksa, K., Frank, H.A., 1972. Bacterial degradation of benzyl isothiocyanate. Appl. Microbiol. 23, 1145–1148.

Vaughn, S., Berhow, M., 2005. Glucosinolate hydrolysis products from various plant sources: pH effects, isolation, and purification. Ind. Crop. Prod. 21, 193–202. https://doi.org/10.1016/j.indcrop.2004.03.004.

Wittstock, U., Kurzbach, E., Steiner, A.M., Stauber, E.J., 2016. Glucosinolate breakdown. Adv. Bot. Res. 80, 125–169. https://doi.org/10.1016/bs.abr.2016.06.006.

Wuensch, C., Lechner, H., Glueck, S.M., Zangger, K., Hall, M., Faber, K., 2013. Asymmetric biocatalytic Cannizzaro-type reaction. ChemCatChem 5, 1744–1748. https://doi.org/10.1002/cctc.201300028.

Yábar, E., Pedreschi, R., Chirinos, R., Campos, D., 2011. Glucosinolate content and myrosinase activity evolution in three maca (*Lepidium meyenii* Walp.) ecotypes during preharvest, harvest and postharvest drying. Food Chem. 127, 1576–1583. https://doi.org/10.1016/j.foodchem.2011.02.021.

Zhang, S.Z., Yang, F., Shao, J.L., Pu, H.M., Ruan, Z.Y., Yang, W.L., Li, H., 2020. The metabolic formation profiles of macamides accompanied by the conversion of glucosinolates in maca (*Lepidium meyenii*) during natural air drying. Int. J. Food Sci. Technol. 55, 2428–2440. https://doi.org/10.1111/ijfs.14493.